

Random lasing action in a polydimethylsiloxane wrinkle induced disordered structure

Zhenhua Shen, Leilei Wu, Shu Zhu, Yuanlin Zheng, and Xianfeng Chen

Citation: [Applied Physics Letters](#) **105**, 021106 (2014); doi: 10.1063/1.4890525

View online: <http://dx.doi.org/10.1063/1.4890525>

View Table of Contents: <http://scitation.aip.org/content/aip/journal/apl/105/2?ver=pdfcov>

Published by the [AIP Publishing](#)

Articles you may be interested in

[Lasing in nanoimprinted two-dimensional photonic crystal band-edge lasers](#)

Appl. Phys. Lett. **102**, 073101 (2013); 10.1063/1.4790646

[Random lasing from localized modes in strongly scattering systems consisting of macroporous titania monoliths infiltrated with dye solution](#)

Appl. Phys. Lett. **97**, 031118 (2010); 10.1063/1.3464962

[Wafer-scale fabrication of polymer distributed feedback lasers](#)

J. Vac. Sci. Technol. B **24**, 3252 (2006); 10.1116/1.2387154

[Thermal behavior of random lasing in dye doped nematic liquid crystals](#)

Appl. Phys. Lett. **89**, 121109 (2006); 10.1063/1.2356087

[Lasing in organic circular grating structures](#)

J. Appl. Phys. **96**, 3043 (2004); 10.1063/1.1776315



AIP | Journal of
Applied Physics

Journal of Applied Physics is pleased to
announce **André Anders** as its new Editor-in-Chief

Random lasing action in a polydimethylsiloxane wrinkle induced disordered structure

Zhenhua Shen, Leilei Wu, Shu Zhu, Yuanlin Zheng, and Xianfeng Chen^{a)}

The State Key Laboratory of Advanced Optical Communication Systems and Networks, Department of Physics and Astronomy, Shanghai Jiao Tong University, Shanghai 200240, China

(Received 19 May 2014; accepted 6 July 2014; published online 17 July 2014)

This paper presents a chip-scale random lasing action utilizing polydimethylsiloxane (PDMS) wrinkles with random periods as disordered medium. Nanoscale wrinkles with long range disorder structures are formed on the oxidized surface of a PDMS slab and confirmed by atomic force microscopy. Light multiply scattered at each PDMS wrinkle-dye interfaces is optically amplified in the presence of pump gain. The shift of laser emission wavelength when pumping at different regions indicates the randomness of the wrinkle period. In addition, a relatively low threshold of about $27 \mu\text{J}/\text{mm}^2$ is realized, which is comparable with traditional optofluidic dye laser. This is due to the unique sinusoidal Bragg-grating-like random structure. Contrast to conventional microfluidic dye laser that inevitably requires the accurate design and implementation of microcavity to provide optical feedback, the convenience in both fabrication and operation makes PDMS wrinkle based random laser a promising underlying element in lab-on-a-chip systems and integrated microfluidic networks. © 2014 AIP Publishing LLC. [<http://dx.doi.org/10.1063/1.4890525>]

Optofluidic dye lasers are of great interest in the past few years for their broad on-chip applications as integrated photonic source elements in micro total analysis systems (μ -TAS).^{1–5} To date, various types of microcavities have been exploited in versatile optofluidic dye lasers to enhance light confinement, including Fabry-Perot (F-P) resonators,^{6,7} microring resonators,^{8,9} distributed feedback (DFB) gratings,^{10–12} optofluidic ring resonators (OFRRs),^{13–16} and microdroplet cavities.^{17–19} Although considerable efforts have been made towards the optimization in microcavity design, accurate manufacture in soft lithography procedures and precise control of liquid flow rates are still of great necessities,^{13,18} which adds enormous complexities in both fabrication and operation.

Contrary to aforementioned microfluidic dye lasers, random laser can be easily achieved in a dye filled microfluidic channel with dispersed TiO_2 nanoparticles despite the absence of an optical cavity, in which the optical feedback is provided by multiple scattering between nanoparticles.²⁰ Apart from similarities in physics mechanism with semiconductor random laser,^{21,22} integrating random laser source onto a miniaturize microfluidic chip provides significant benefits such as low costs, easy fabrication, portability, and high degrees of functionalities. Furthermore, random laser with low spatial coherence may also perform as a potential illumination source for on-chip speckle-free laser imaging.²³ Recently, the fusion of optofluidics and random structures offers a new route for on-chip random laser source integration. Bhaktha *et al.* demonstrated an optofluidic random laser based on the inherent disorder of snake-shaped polydimethylsiloxane (PDMS) channel due to the limited accuracy of soft lithography which largely reduces the demands of high standard fabrication techniques.²⁴ The research opens the door for exploration in optofluidic random laser, and

thereafter, much attention has been paid to on-chip random laser investigation due to its mirrorless character with easy fabrication processes.

In this work, we introduce an on chip random laser based on PDMS wrinkle induced disordered structure, which further simplifies the random laser fabrication process by getting rid of lithography procedures. The wrinkles are formed by plasma oxidation of pre-stretched PDMS surface and subsequent relaxation. The structure of the demonstrated random laser is created by sandwiching a thin dye layer between a flat PDMS stamp and a wrinkled PDMS slab. Due to the inherent disorder of the wrinkles which is caused by non-uniform relaxation of the plasma treated PDMS stamp, multiple scattering can be effectively enhanced. As a result, lasing action with a relatively low threshold can be established when the optical gain is larger than the optical loss without a resonance mechanism. The sensitivity of emission spectrum with respect to pump position perturbation also indicates the randomness of the wrinkle period. The unique one dimensional random structure can also be applied to select the desire mode of the emission spectrum via active spatial control of the pump laser, which offers a new platform to investigate random laser physics.^{25,26} More importantly, the chip-scale disorder-based light source delivers the possibility in microfluidic laser source integration as well as in related optofluidic laser applications.

The wrinkled PDMS surface is created by a previously developed and commonly used technique for polymeric surface modification through oxygen plasma surface treatment.^{27,28} The preparation procedure is schematically illustrated in Fig. 1. Briefly, PDMS is first mixed with its curing agent at a weight ratio of 10:1, followed by curing at 65°C for about 2 h. Then the PDMS slab is stretched uniaxially by a custom-designed stretching device to a maximum strain of ε (60%). Thereafter, the prepared sample is placed into the plasma chamber and exposed to oxygen plasma (PDC-002, Harrick Plasma, High level power) for

^{a)}Author to whom correspondence should be addressed. Electronic mail: xfchen@sjtu.edu.cn

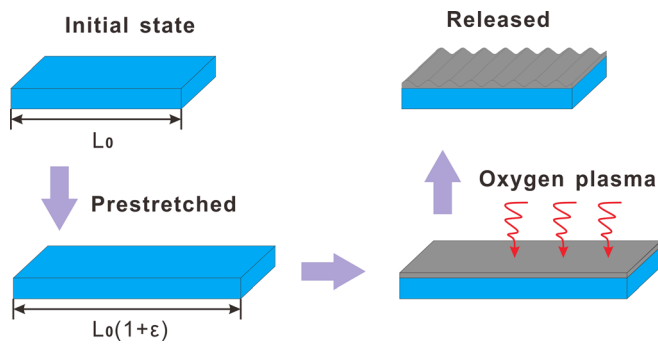


FIG. 1. Schematic illustration of preparation procedures for wrinkled PDMS surface formation.

90 min to generate a uniform silicate-like hard skin at the surface of the PDMS slab. Finally, the applied strain is gradually released and the buckled surface is formed owing to the modulus mismatch between the hard skin and the soft PDMS substrate. Due to the inevitably non-uniform releasing speed of the strained PDMS slab, the buckled surface shows the random structure in both wrinkle period and amplitude as shown in Figs. 2(a) and 2(b). The wrinkle period is around $1\ \mu\text{m}$ while the wrinkle amplitude is around 300 nm as measured by atomic force microscopy (AFM). Since the sample is also deformed in the transverse direction when the strain is applied, some cracks can be found along the wrinkle period when the strain is released. But they do not affect the experiment thanks to their relative low density distribution compared with that of wrinkles.

The prepared PDMS slice was then cut at the dimension of around $20 \times 15 \times 1.5$ (mm) in our experiment. For gain medium implementation, Rhodamine 6 G (R6G) is dissolved in ethylene glycol with a concentration of 2 mM. A droplet of ethylene glycol dye solution is deposited onto another surface of a flat PDMS and then covered by the wrinkled PDMS slab as depicted in Fig. 2(c). Finally, by slightly pressing the wrinkled PDMS stamp, a thin film of R6G dye can be confined uniformly between the flat PDMS slab and the

wrinkled PDMS stamp. When the random laser structure is optically pumped, unidirectional laser can be collected at the edge of the PDMS chip. The sandwich structure of the wrinkle induced random laser is illustrated in Fig. 2(d). This unique PDMS random wrinkle structure is similar with one dimensional random laser model proposed previously and has already been investigated theoretically.^{29,30}

The random laser chip is pumped by a Nd:YAG laser (532 nm center wavelength, 4 ns pulse width, and 20 Hz repetition rate). The chip is placed on a three-dimensional translation stage so that the pumping position can be easily tuned. The laser emission is coupled from one edge of the chip and then transmitted to the optical spectrometer (SR500, Andor, resolution 0.09 nm) by a pair of convex lens followed by a long-pass filter which aims at the removal of the green pump light.

Figure 3(a) shows the emission spectrum of the random laser at various pump pulse intensities. Light is multiply scattered at each dye-PDMS wrinkle interface. When the pump energy is low, the multiple scattering cannot support efficient optical feedback, leading to spontaneous emission of the R6G in ethylene glycol solution. As the pump intensity increases, optical amplification is achieved and accompanied by the narrow linewidth of the emission spectrum. Besides the simplicity in fabrication and operation, the random laser also performs well in terms of the lasing threshold. Figure 3(b) depicts the output intensity versus pump pulse intensity. The nonlinear relationship between the laser emission intensity and pump pulse intensity can be established, which indicates the lasing threshold of $27.0\ \mu\text{J}/\text{mm}^2$. Strikingly, in spite of the microcavity to provide optical feedback, the lasing threshold is comparable with traditional microfluidic dye lasers.^{16,31} The typical laser linewidth can be as narrow as 1 nm when the pump pulse intensity is much larger than the threshold, showing the coherent optical feedback provided by multiple scattering of the wrinkled architecture.^{22,32} Moreover, the unidirectional random laser emission along the PDMS wrinkle period as depicted in the

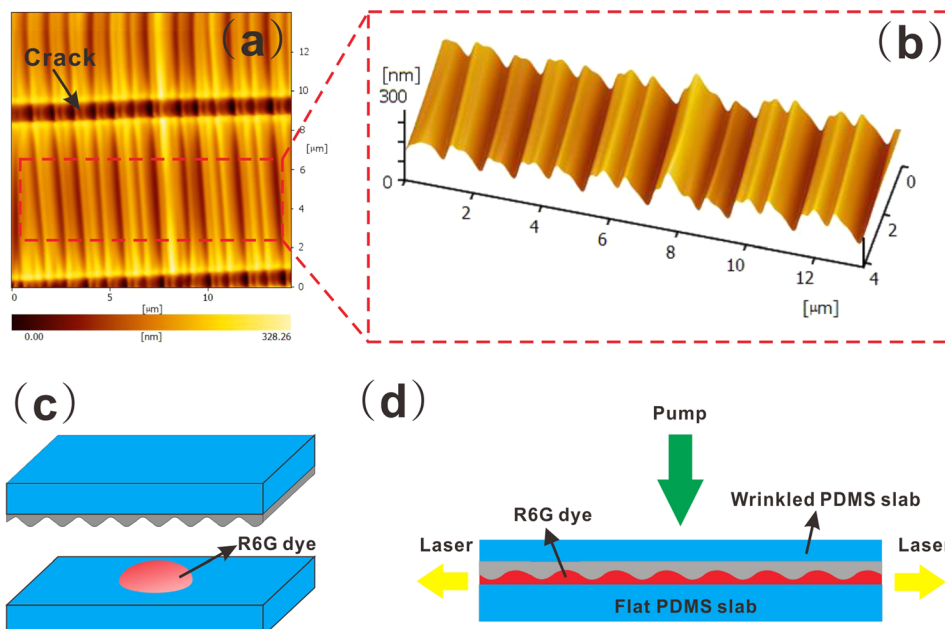


FIG. 2. (a) AFM image of PDMS surface wrinkle patterns created by plasma treatment. (b) Partial magnified picture of the buckled PDMS surface. The non-uniform random wrinkle wavelength and amplitude is around $1\ \mu\text{m}$ and 300 nm, respectively. (c) Preparation of the sandwich structure for random lasing. A droplet of ethylene glycol dye solution is first deposited on to the surface of a flat PDMS stamp and then confined with a wrinkled PDMS slab. (d) The front-view diagram of the sandwich random lasing architecture.

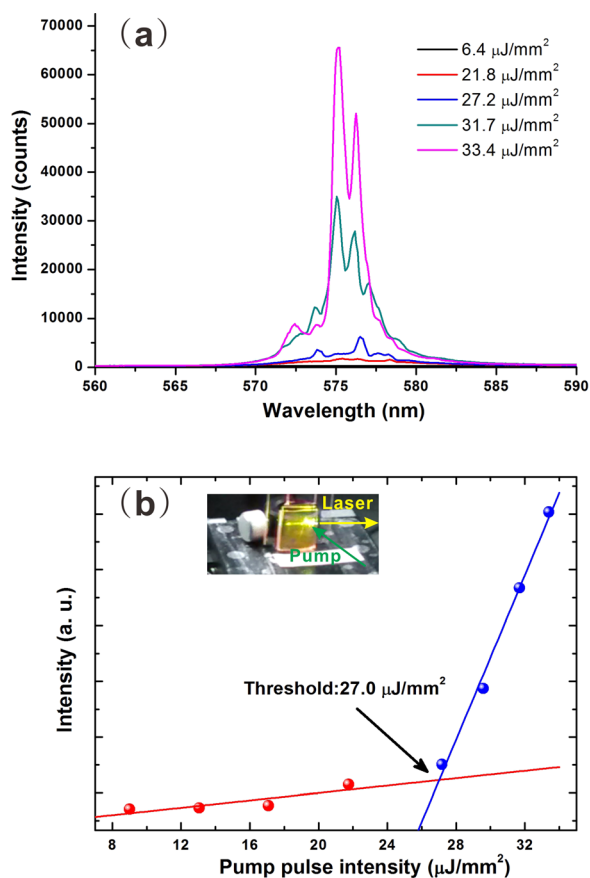


FIG. 3. (a) Typical emission spectra of random laser at various pump pulse intensity. (b) Output intensity of the random laser as a function of the incident pump pulse intensity. The lasing threshold is determined to be $27.0 \mu\text{J}/\text{mm}^2$. Inset image: a random lasing chip used in the experiment.

inset picture of Fig. 3(b) offers a great opportunity in laser related practical applications.

In order to show the stability of the laser emission, lasing spectra at a randomly selected position have been recorded at different time with the pump energy of around $29.3 \mu\text{J}/\text{mm}^2$, as shown in Fig. 4. The output laser is normalized in order to distinguish whether the peak shifts or not. Although the emission spectrum profiles are varied due to

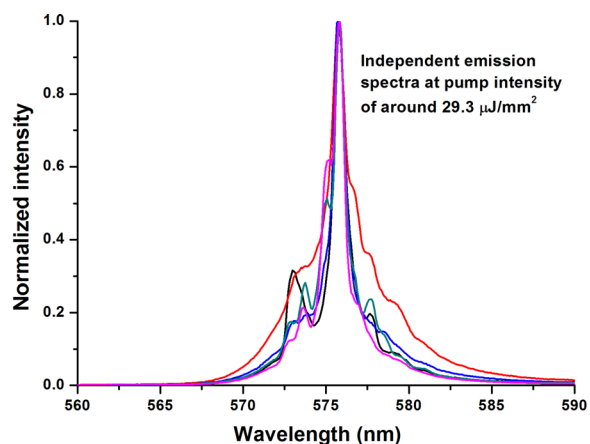


FIG. 4. Normalized emission spectra at the same position with the pump intensity of around $29.3 \mu\text{J}/\text{mm}^2$. The spectra show the same peak in spite of the different emission curve profile that might be caused by pump pulse energy fluctuations.

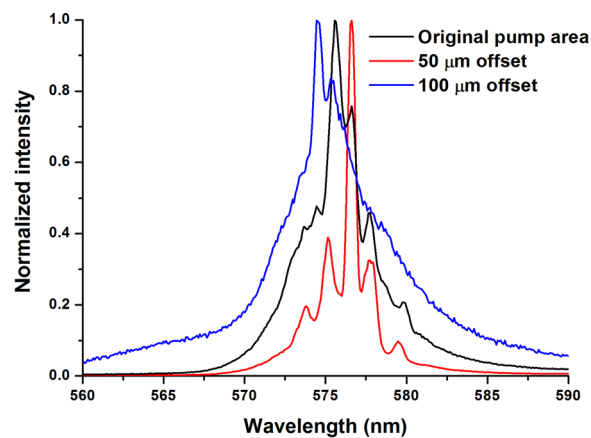


FIG. 5. The emission lasing spectra when pumped at different positions. Slight change in the pump area results in different lasing peak emission.

the energy fluctuations of pump pulses, the peak wavelength remains in the dominant position of around 575.8 nm . Thus a stable emission of random laser can be obtained in disordered wrinkle structures.

To further confirm the randomness of the wrinkle structure, we slightly change the pump position by horizontally shifting the random laser chip. Figure 5 illustrates the lasing wavelength shifts at different pump positions. In spite of a relative small displacement of around $50 \mu\text{m}$ each time, about 50 wrinkle periods have been replaced according to the AFM image in Fig. 2. Therefore, different pump regions correspond to different wrinkle configuration, which leads to the drift of lasing peak in the emission spectrum. In the experiment, $100 \mu\text{m}$ offset of the pumping spot could induce a 2 nm peak shift in the emission spectrum. Since the output laser shows a great spatial dependence with pump position, the emission spectrum can be tuned by varying different pumping areas. Besides, the strong emission spectrum sensitivity with respect to different pump areas is not available in traditional microfluidic dye laser systems, which makes the wrinkle based random laser a promising component in microfluidic sensing applications.

In summary, a chip-scale PDMS wrinkle based random laser without using traditional lithography techniques is demonstrated in this paper, providing flexibility and simplicity for large scale production of the device. The disordered wrinkle structure multiply scatters the light and results in optical amplification even without microcavity structure when the pump is introduced. The relatively low threshold that is comparable with conventional microfluidic dye laser is achieved. The emission wavelength can be sensitively tuned when pumping at different regions, which also confirms the randomness of the wrinkle period. In addition, the emission sensitivity against pump area also indicates the wrinkle based random laser a promising platform for bio-chemical and bio-sensing applications. We envision that the fusion of this compact random laser with a large variety of state-of-the-art microfluidic components can create much more functionality in lab-on-a-chip systems.

This work was supported by the National Basic Research Program of China (No. 2011CB808101), the National Natural Science Foundation of China (No.

61125503), and the Foundation for Development of Science and Technology of Shanghai (No. 13JC1408300).

- ¹D. Psaltis, S. R. Quake, and C. Yang, *Nature* **442**, 381–386 (2006).
- ²Z. Li and D. Psaltis, *Microfluid. Nanofluid.* **4**, 145–158 (2008).
- ³Y. Chen, L. Lei, K. Zhang, J. Shi, L. Wang, H. Li, X. M. Zhang, Y. Wang, and H. L. W. Chan, *Biomicrofluidics* **4**, 043002 (2010).
- ⁴X. D. Fan and I. M. White, *Nat. Photonics* **5**, 591–597 (2011).
- ⁵C. Monat, P. Domachuk, C. Grillet, M. Collins, B. J. Eggleton, M. Cronin-Golomb, S. Mutzenich, T. Mahmud, G. Rosengarten, and A. Mitchell, *Microfluid. Nanofluid.* **4**, 81–95 (2008).
- ⁶B. Helbo, A. Kristensen, and A. Menon, *J. Micromech. Microeng.* **13**, 307–311 (2003).
- ⁷D. V. Vezenov, B. T. Mayers, R. S. Conroy, G. M. Whitesides, P. T. Snee, Y. Chan, D. G. Nocera, and M. G. Bawendi, *J. Am. Chem. Soc.* **127**, 8952–8953 (2005).
- ⁸Z. Li, Z. Zhang, A. Scherer, and D. Psaltis, *Digest of the LEOS Summer Topical Meetings* (2007), pp. 70–71.
- ⁹Z. Shen, Y. Zou, and X. Chen, *Sci. China: Technol. Sci.* **56**, 594–597 (2013).
- ¹⁰M. Gersborg-Hansen and A. Kristensen, *Opt. Express* **15**, 137–142 (2007).
- ¹¹Z. Y. Li, Z. Y. Zhang, T. Emery, A. Scherer, and D. Psaltis, *Opt. Express* **14**, 696–701 (2006).
- ¹²W. Z. Song, A. E. Vasdekis, and D. Psaltis, “Organic photonic materials and devices XII,” *SPIE Proc.* **7599**, 75991–75998 (2010).
- ¹³W. Lee, H. Li, J. D. Suter, K. Reddy, Y. Sun, and X. Fan, *Appl. Phys. Lett.* **98**, 061103 (2011).
- ¹⁴S. Lacey, I. M. White, Y. Sun, S. I. Shopova, J. M. Cupps, P. Zhang, and X. D. Fan, *Opt. Express* **15**, 15523–15530 (2007).
- ¹⁵S. I. Shopova, H. Zhou, X. Fan, and P. Zhang, *Appl. Phys. Lett.* **90**, 221101 (2007).
- ¹⁶J. D. Suter, W. Lee, D. J. Howard, E. Hoppmann, I. M. White, and X. D. Fan, *Opt. Lett.* **35**, 2997–2999 (2010).
- ¹⁷W. Lee, Y. H. Luo, Q. R. Zhu, and X. D. Fan, *Opt. Express* **19**, 19668–19674 (2011).
- ¹⁸S. K. Tang, Z. Li, A. R. Abate, J. J. Agresti, D. A. Weitz, D. Psaltis, and G. M. Whitesides, *Lab Chip* **9**, 2767–2771 (2009).
- ¹⁹M. Tanyeri, R. Perron, and I. M. Kennedy, *Opt. Lett.* **32**, 2529–2531 (2007).
- ²⁰K. C. Vishnubhatla, J. Clark, G. Lanzani, R. Ramponi, R. Osellame, and T. Virgili, *Appl. Opt.* **48**, G114–G118 (2009).
- ²¹D. S. Wiersma, *Nat. Phys.* **4**, 359–367 (2008).
- ²²H. Cao, Y. G. Zhao, S. T. Ho, E. W. Seelig, Q. H. Wang, and R. P. H. Chang, *Phys. Rev. Lett.* **82**, 2278–2281 (1999).
- ²³B. Redding, M. A. Choma, and H. Cao, *Nat. Photonics* **6**, 355–359 (2012).
- ²⁴B. N. Shivakiran Bhaktha, N. Bachelard, X. Noblin, and P. Sebbah, *Appl. Phys. Lett.* **101**, 151101 (2012).
- ²⁵N. Bachelard, J. Andreasen, S. Gigan, and P. Sebbah, *Phys. Rev. Lett.* **109**, 033903 (2012).
- ²⁶N. Bachelard, S. Gigan, X. Noblin, and P. Sebbah, *Nat. Phys.* **10**, 426–431 (2014).
- ²⁷C. Harrison, C. M. Stafford, W. Zhang, and A. Karim, *Appl. Phys. Lett.* **85**, 4016 (2004).
- ²⁸C. M. Stafford, C. Harrison, K. L. Beers, A. Karim, E. J. Amis, M. R. VanLandingham, H. C. Kim, W. Volksen, R. D. Miller, and E. E. Simonyi, *Nature Mater.* **3**, 545–550 (2004).
- ²⁹X. Y. Jiang and C. M. Soukoulis, *Phys. Rev. B* **59**, 6159–6166 (1999).
- ³⁰Z.-Q. Zhang, *Phys. Rev. B* **52**, 7960–7964 (1995).
- ³¹Y. Yang, A. Q. Liu, L. Lei, L. K. Chin, C. D. Ohl, Q. J. Wang, and H. S. Yoon, *Lab Chip* **11**, 3182–3187 (2011).
- ³²H. Cao, *Wave Random Media* **13**, R1–R39 (2003).